

# Chemistry of Unsaturated Group 6 Metal Complexes with Bridging Hydroxy and Methoxycarbyne Ligands. 1. Synthesis, Structure, and Bonding of 30-Electron Complexes

M. Esther García,<sup>†</sup> Daniel García-Vivó,<sup>†</sup> Miguel A. Ruiz,<sup>\*,†</sup> Santiago Alvarez,<sup>‡</sup> and Gabriel Aullón<sup>‡</sup>

Departamento de Química Orgánica e Inorgánica/IUQOEM, Universidad de Oviedo, E-33071 Oviedo, Spain, and Departamento de Química Inorgánica, Universidad de Barcelona, E-08028 Barcelona, Spain

Received June 8, 2007

The new cationic alkoxy and hydroxycarbyne complexes  $[M_2Cp_2(\mu-COR)(\mu-PR'_2)_2]BF_4$  ( $Cp = \eta^5-C_5H_5$ ;  $M = W$ ,  $R = Me$ ,  $R' = Ph$ ;  $M = Mo$ ,  $R = Me$  and  $H$ ,  $R' = Et$ ) and  $[Mo_2Cp_2(\mu-COR)(\mu-COR')(\mu-PCy_2)]BF_4$  ( $R = Me$ ;  $R' = H$ ,  $Me$ ,  $Et$ ) are obtained in high yield by the reaction of the corresponding neutral monocarbonyl precursors with either  $[Me_3O]BF_4$  or  $HBF_4 \cdot OEt_2$  in dichloromethane. While the methoxycarbyne complexes are stable at room temperature, the analogous hydroxycarbyne species are thermally unstable, and above ca. 253 K they experience a hydrogen migration from oxygen to metal, to give the new hydride carbonyl complexes  $[Mo_2Cp_2(H)(\mu-PET_2)_2(CO)]BF_4$  and  $[Mo_2Cp_2(H)(\mu-COMe)(\mu-PCy_2)(CO)]BF_4$  as major products. The electronic structure and bonding in some of these face-sharing bioctahedral complexes were studied by means of density functional theory. These calculations allow us to describe the intermetallic interaction present in the carbonyl-bridged 30-electron complexes by a configuration of type  $\sigma^2\delta^4$ , with the  $\delta$  orbitals being involved in  $\pi$  back-bonding to the carbonyl bridges. Upon methylation of the latter ligands, these  $\delta$ -bonding orbitals become more delocalized over the  $Mo_2C$ - (carbyne) triangle and constitute the  $\pi$ -bonding component of the metal–carbyne bond. Therefore, a partial reduction of the direct metal–metal overlap occurs upon formation of these methoxycarbyne complexes, which still retain some multiplicity in the corresponding C–O bonds. The topological analysis of the electron density under the AIM scheme supports the above description of the Mo–Mo, Mo–C, and C–O bonds in these complexes.

## Introduction

Since the discovery of the first metal–alkylidyne complexes at E. O. Fischer's laboratory in 1973,<sup>1</sup> this area within organometallic chemistry has developed tremendously.<sup>2</sup> These complexes are of interest not only because of their great reactivity but also for their relevance in the context of some important industrial reactions such as the Fischer–Tropsch process and other metal-catalyzed hydrogenations of CO,<sup>3,4</sup> or the alkyne metathesis.<sup>5</sup>

Compared to the extensively developed chemistry of complexes containing the alkylidyne moiety CR ( $R = \text{alkyl, aryl}$ ),

relatively little work has been carried out on the corresponding alkoxy-substituted carbyne (COR) or hydroxycarbyne (COH) complexes, even though Shriver and co-workers reported the first complex displaying a bridging alkoxy-carbyne ligand (obtained by O-alkylation of a bridging carbonyl in the anion  $[Fe_3(CO)_{11}(H)]^-$ ) only 2 years after the pioneering work of Fischer.<sup>6</sup> Besides a few complexes displaying terminal coordination of the COR moiety,<sup>7</sup> most of the alkoxy-carbyne complexes described so far contain this ligand acting as a bridging group (in a  $\mu_2$  or  $\mu_3$  fashion) on electron-precise di- or trinuclear metal centers, and it is on these substrates that the reactivity of the alkoxy-carbyne ligand has been mostly investigated.<sup>8</sup> As a result, little is known of the behavior of these ligands when bridging multiple metal–metal bonds.

The chemistry of hydroxycarbyne (COH) complexes is even more undeveloped than that of the alkoxy-carbyne complexes, due to the lack of available compounds with enough thermal stability. In fact the only stable complexes of this type so far reported are the unsaturated cations  $[Mo_2Cp_2(\mu-COH)(\mu-PCy_2)_2]^+$ ,<sup>9</sup>  $[W_2Cp_2(\mu-COR)(\mu-L_2)(CO)_2]^+$  ( $Cp = \eta^5-C_5H_5$ ;  $L_2 = Ph_2PCH_2PPh_2$ ,  $Me_2PCH_2PMe_2$ ;  $R = H$ ,  $Me$ ),<sup>10</sup> and  $[M_2Cp_2(\mu-COR)(\mu-PPh_2)_2]^+$  ( $M = Mo$ ,  $W$ ;  $R = H$ ,  $Me$ ),<sup>11</sup> all of them

<sup>†</sup> Universidad de Oviedo.

<sup>‡</sup> Universidad de Barcelona.

(1) Fischer, E. O.; Kreis, G.; Kreiter, C. G.; Müller, J.; Hüttner, G.; Lorentz, H. *Angew. Chem., Int. Ed. Engl.* **1973**, *12*, 564.

(2) See for example: (a) Stone, F. G. A. *Leaving No Stone Unturned. Pathways in Organometallic Chemistry*; American Chemical Society: Washington, DC, 1993. (b) Fischer, H.; Hoffmann, P.; Kreissl, F. R.; Schrock, R. R.; Schubert, U.; Weiss, K. *Carbyne Complexes*; VCH: Weinheim, Germany, 1988. (c) Mays, A.; Hoffmeister, H. *Adv. Organomet. Chem.* **1991**, *32*, 259. (d) Angelici, R. J.; Heesook, K. P. *Adv. Organomet. Chem.* **1987**, *27*, 51. (e) Stone, F. G. A. *Angew. Chem., Int. Ed. Engl.* **1984**, *23*, 89.

(3) (a) Maitlis, P. M. *J. Organomet. Chem.* **2004**, *689*, 4366. (b) Maitlis, P. M. *J. Mol. Catal. A* **2003**, *204–205*, 55. (c) Dry, M. E. *Catal. Today* **2002**, *71*, 227. (d) Campbell, I. M. *Catalysis at Surfaces*; Chapman and Hall: New York, 1988. (e) Bell, A. T. *Catal. Rev. Sci. Eng.* **1981**, *23*, 203.

(4) Nicholas, K. M. *Organometallics* **1982**, *1*, 1713.

(5) For some recent reviews see: (a) Mori, M.; Kitamura, K. In *Comprehensive Organometallic Chemistry III*; Crabtree, R. H., Mingos, D. M. P., Eds.; Elsevier: Oxford, UK, 2007; Vol. 11, Chapter 8. (b) Mortreux, A.; Coutelier, O. *J. Mol. Catal. A* **2006**, *254*, 96. (c) Schrock, R. R. *Chem. Commun.* **2005**, 2773.

(6) Shriver, D. F.; Lehman, D.; Strobe, D. *J. Am. Chem. Soc.* **1975**, *97*, 1594.

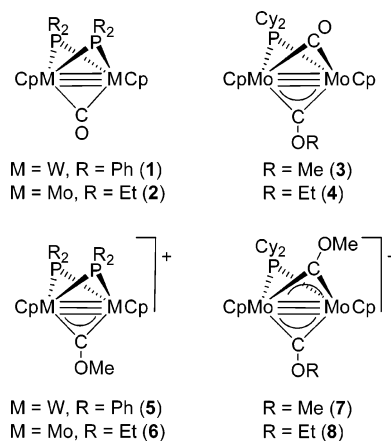
(7) (a) Stone, K. C.; Jamison, G. M.; White, P. S.; Templeton, J. L. *Organometallics* **2003**, *22*, 3083. (b) Stone, K. C.; White, P. S.; Templeton, J. L. *J. Organomet. Chem.* **2003**, *684*, 13. (c) Peters, J. C.; Odon, A. L.; Cummins, C. C. *Chem. Commun.* **1997**, 1995. (d) Carnahan, E. M.; Protasiewicz, J. D.; Lippard, S. J. *Acc. Chem. Res.* **1993**, *26*, 90. (e) Jamison, G. M.; White, P. S.; Templeton, J. L. *Organometallics* **1991**, *10*, 1954.

prepared in our laboratory. The related methoxycarbyne complex cations are more robust thermally, but still they are the first binuclear alkoxy-carbyne complexes with electron counts of 30 or 32, and the chemistry of all these species remains largely unexplored. We have noted previously that the study of the reactivity of hydroxy- and alkoxy-carbyne ligands at unsaturated binuclear centers might be of interest not only because of the unusual transformations that can be induced by the coexistence of different multiple bonds (metal–metal and metal–carbon) in the same substrate but also in the context of the metal-catalyzed hydrogenation processes of carbon monoxide.<sup>10</sup>

Apart from their interest as synthetic intermediates, the unsaturated dimolybdenum and ditungsten complexes mentioned above, for which we can formulate metal–metal bond orders (BO) of 2 and 3 according to the effective atomic number (EAN) rule, are good candidates for theoretical studies as well, both because of the presence of multiple metal–metal bonding and because of the presence of the alkoxy-carbyne bridge itself. Indeed the nature of the intermetallic interaction in unsaturated binuclear transition metal complexes has been the subject of intense debate, and a lot of experimental and theoretical research has been carried out, but it still remains an active area of research.<sup>13</sup> Special problems are found in complexes containing bridging  $\pi$ -acid ligands, since the metal–metal interaction is extensively delocalized over the bridges.<sup>14</sup> This obviously can be the case of the hydroxycarbyne or alkoxy-carbyne ligands, but this matter has not been previously studied using modern quantum mechanical methods. To our knowledge, the only previous study on the electronic structure and bonding of an alkoxy-carbyne complex was carried out some years ago by Farrugia and Aitchison using extended-Hückel methods.<sup>15</sup>

In this paper we report the synthesis and structural characterization of new unsaturated hydroxy and alkoxy-carbyne

Chart 1



complexes having formally triple metal–metal bonds. These have been prepared via O-alkylation or protonation of the bridging carbonyl ligands in the neutral complexes  $[W_2Cp_2(\mu-PPh_2)_2(\mu-CO)]$  (1),<sup>16</sup>  $[Mo_2Cp_2(\mu-PtEt_2)_2(\mu-CO)]$  (2),<sup>16</sup> and  $[Mo_2Cp_2(\mu-COR)(\mu-PCy_2)(\mu-CO)]$  [R = Me (3), Et (4)].<sup>17</sup> Although the reactivity of the new cationic complexes will be reported separately, we here include the results of a complete study of the electronic structure and bonding in these complexes based on density functional theory (DFT) calculations, with special attention given to the nature of the intermetallic interaction and the changes induced upon alkylation of the carbonyl ligands. This computational study will also give us a basis for the interpretation of the reaction patterns of these complexes.

Some of the synthetic work here discussed, as well as some unusual transformations experienced by the new unsaturated cations (that involve *inter alia* the formation and cleavage of C–C, C–O, and O–H bonds), was previously reported in a short communication.<sup>18</sup>

## Results and Discussion

**Synthesis and Structural Characterization of New Cationic Methoxycarbyne Complexes.** The neutral compounds 1–4 are methylated easily at the oxygen atom of their carbonyl bridges upon reaction with  $[Me_3O]BF_4$  in dichloromethane solution, to give the new cationic methoxycarbyne complexes  $[M_2Cp_2(\mu-COMe)(\mu-PR_2)_2]BF_4$  [M = W, R = Ph (5); M = Mo, R = Et (6)] and  $[Mo_2Cp_2(\mu-COMe)(\mu-COR)(\mu-PCy_2)]BF_4$  [R = Me (7), Et (8)], respectively, in high yields (Chart 1). All these 30-electron complexes, for which we can formulate a metal–metal triple bond according to the EAN rule, exhibit a face-sharing bioctahedral geometry, with the bridging positions being occupied by either two phosphide and one methoxycarbyne or one phosphide and two alkoxy-carbyne ligands.

Spectroscopic data for the bis(phosphide) complexes 5 and 6 (Table 1 and Experimental Section) are similar to those previously reported by us for the triflate salt of compound 5,  $[W_2Cp_2(\mu-COMe)(\mu-PPh_2)_2](CF_3SO_3)$ , a complex obtained through the slower reaction of 1 with  $CF_3SO_3Me$  and characterized through a single-crystal X-ray study.<sup>11</sup> Therefore we can propose for the cation in compounds 5 and 6 a structure essentially identical to that determined for the above triflate salt,

(8) For some studies of reactivity of alkoxy-carbyne-bridged compounds see: (a) Hersh, W. H.; Fong, R. H. *Organometallics* **2005**, *24*, 4179. (b) Peters, J. C.; Odon, A. L.; Cummins, C. C. *Chem. Commun.* **1997**, 1995. (c) Bronk, B. S.; Protasiewicz, J. D.; Pence, L. E.; Lippard, S. J. *Organometallics* **1995**, *14*, 2177. (d) Seyferth, D.; Ruschke, D. P.; Davis, W. H. *Organometallics* **1994**, *13*, 4695. (e) Chi, Y.; Chuang, S. H.; Chen, B.-F.; Peng, S.-M.; Lee, G.-H. *J. Chem. Soc., Dalton Trans.* **1990**, 3033. (f) Friedman, A. E.; Ford, P. C. *J. Am. Chem. Soc.* **1989**, *111*, 551. (g) Keister, J. B. *Polyhedron* **1988**, *7*, 847. (h) Friedman, A. E.; Ford, P. C. *J. Am. Chem. Soc.* **1986**, *108*, 7851. (i) Farrugia, L. J.; Miles, A. D.; Stone, F. G. A. *J. Chem. Soc., Dalton Trans.* **1985**, 2437. (j) Beanan, L. R.; Keister, J. B. *Organometallics* **1985**, *4*, 1713. (k) Nuel, D.; Dahan, F.; Mathieu, R. *J. Am. Chem. Soc.* **1985**, *107*, 1658. (l) Shapley, J. R.; Yeh, W.-Y.; Churchill, M. R.; Li, Y.-J. *Organometallics* **1985**, *4*, 1898. (m) Green, M.; Mead, K. A.; Mills, R. M.; Salter, I. D.; Stone, F. G. A.; Woodward, P. J. *J. Chem. Soc., Chem. Commun.* **1982**, 51.

(9) Alvarez, M. A.; García, M. E.; Martínez, M. E.; Ramos, A.; Ruiz, M. A.; Sáez, D.; Vaissermann, J. *Inorg. Chem.* **2006**, *45*, 6965.

(10) (a) Alvarez, M. A.; García, M. E.; Riera, V.; Ruiz, M. A.; Robert, F. *Organometallics* **2002**, *21*, 1177. (b) Alvarez, M. A.; García, M. E.; Riera, V.; Ruiz, M. A. *Organometallics* **1999**, *18*, 634. (c) Alvarez, M. A.; Bois, C.; García, M. E.; Riera, V.; Ruiz, M. A. *Angew. Chem., Int. Ed. Engl.* **1996**, *35*, 102.

(11) García, M. E.; Riera, V.; Rueda, M. T.; Ruiz, M. A.; Halut, S. J. *Am. Chem. Soc.* **1999**, *121*, 1960.

(12) Cotton, F. A.; Murillo, C. A.; Walton, R. A. *Multiple Bonds between Metal Atoms*, 3rd ed.; Springer Science: New York, 2005.

(13) See for example: (a) Brynda, M.; Gagliardi, L.; Widmark, P.-O.; Power, P. P.; Roos, B. O. *Angew. Chem., Int. Ed.* **2006**, *45*, 3804. (b) Radius, U.; Breher, F. *Angew. Chem., Int. Ed.* **2006**, *45*, 3006. (c) Nguyen, T.; Sutton, A. D.; Brynda, M.; Fettingner, J. C.; Long, G. J.; Power, P. P. *Science* **2005**, *310*, 844.

(14) For some representative studies on this subject see: (a) Wang H.; Xie, Y.; King, R. B.; Schaefer, H. F., III. *Inorg. Chem.* **2006**, *45*, 3384. (b) Kenny, J. P.; King, R. B.; Schaefer, H. F., III. *Inorg. Chem.* **2001**, *40*, 900. (c) Xie, Y.; Schaefer, H. F., III; King, R. B. *J. Am. Chem. Soc.* **2000**, *122*, 8746. (d) Low, A. A.; Hall, M. B. *Inorg. Chem.* **1993**, *32*, 3880. (e) Low, A. A.; Kunze, K. L.; MacDougall, P. J.; Hall, M. B. *Inorg. Chem.* **1991**, *30*, 1079.

(15) Aitchison, A.; Farrugia, L. J. *Organometallics* **1987**, *6*, 819.

(16) García, M. E.; Riera, V.; Ruiz, M. A.; Rueda, M. T.; Sáez, D. *Organometallics* **2002**, *21*, 5515.

(17) García, M. E.; Melón, S.; Ramos, A.; Riera, V.; Ruiz, M. A.; Belletti, D.; Graiff, C.; Tiripicchio, A. *Organometallics* **2003**, *22*, 1983.

(18) Alvarez, C. M.; Alvarez, M. A.; García, M. E.; García-Vivó, D.; Ruiz, M. A. *Organometallics* **2005**, *24*, 4122.

**Table 1. Selected NMR Data for New Compounds<sup>a</sup>**

compound	$\delta_P$	$\delta_{\mu-C}$ ( $J_{CP}$ )
[W <sub>2</sub> Cp <sub>2</sub> ( $\mu$ -COMe)( $\mu$ -PPh <sub>2</sub> ) <sub>2</sub> ]BF <sub>4</sub> ( <b>5</b> )	191.7 <sup>b</sup>	
[Mo <sub>2</sub> Cp <sub>2</sub> ( $\mu$ -COMe)( $\mu$ -PEt <sub>2</sub> ) <sub>2</sub> ]BF <sub>4</sub> ( <b>6</b> )	262.2	367.9(14)
[Mo <sub>2</sub> Cp <sub>2</sub> ( $\mu$ -COMe) <sub>2</sub> ( $\mu$ -PCy <sub>2</sub> )]BF <sub>4</sub> ( <b>7</b> )	264.2	366.0(13)
[Mo <sub>2</sub> Cp <sub>2</sub> ( $\mu$ -COEt)( $\mu$ -COMe)( $\mu$ -PCy <sub>2</sub> )]BF <sub>4</sub> ( <b>8</b> )	263.8	365.7(13)
[Mo <sub>2</sub> Cp <sub>2</sub> ( $\mu$ -COH)( $\mu$ -PEt <sub>2</sub> ) <sub>2</sub> ]BF <sub>4</sub> ( <b>9</b> )	256.7 <sup>c</sup>	368.9(11) <sup>d</sup>
[Mo <sub>2</sub> Cp <sub>2</sub> ( $\mu$ -COH)( $\mu$ -COMe)( $\mu$ -PCy <sub>2</sub> )]BF <sub>4</sub> ( <b>10</b> )	261.5 <sup>e</sup>	365.8(13) <sup>e</sup>
[Mo <sub>2</sub> Cp <sub>2</sub> (H)( $\mu$ -PEt <sub>2</sub> )(CO)]BF <sub>4</sub> ( <b>11</b> )	285.4 <sup>d</sup>	259.8(7) <sup>d</sup>
[Mo <sub>2</sub> Cp <sub>2</sub> (H)( $\mu$ -COMe)( $\mu$ -PCy <sub>2</sub> )(CO)]BF <sub>4</sub> ( <b>12</b> )	294.5 <sup>c</sup>	

<sup>a</sup> Recorded in CD<sub>2</sub>Cl<sub>2</sub> solution at 290 K and 121.50 (<sup>31</sup>P) or 75.47 (<sup>13</sup>C) MHz, unless otherwise stated;  $\delta$  in ppm relative to internal TMS (<sup>13</sup>C) or external 85% aqueous H<sub>3</sub>PO<sub>4</sub> (<sup>31</sup>P);  $J$  in Hz. <sup>b</sup>  $J(^{31}\text{P}-^{183}\text{W}) = 363$ .

<sup>c</sup> Recorded at 243 K. <sup>d</sup> Recorded at 213 K. <sup>e</sup> Recorded at 233 K.

with the methoxyl substituent of the carbyne ligand placed in the plane defined by the metal atoms and the bridgehead carbon (Chart 1), a common structural feature of bridging alkoxycarbyne ligands.<sup>10b</sup>

The <sup>31</sup>P NMR spectra of compounds **5** and **6** show highly deshielded resonances (191.7 and 262.2 ppm, respectively), this being a characteristic of 30-electron dimolybdenum and ditungsten complexes having dialkyl- or diarylphosphide bridges.<sup>9,16–19</sup> The great difference in their chemical shifts (ca. 70 ppm) can be mainly attributed to the distinct deshielding effect of the metal (tungsten vs molybdenum) and, to a lesser extent, to the higher deshielding influence of the bulkier Cy substituents (compared to phenyl) on the phosphorus atom.<sup>16</sup> On the other hand, the bridging methoxycarbyne ligands in **5** and **6** give rise to a characteristic highly deshielded <sup>13</sup>C NMR resonance at ca. 370 ppm, a shift similar to those reported for other complexes displaying bridging alkoxycarbyne ligands.<sup>8,11,17</sup> In addition, these compounds were found to exhibit dynamic behavior in solution, as deduced in each case from the presence in the <sup>1</sup>H and <sup>13</sup>C NMR spectra of just one resonance for both cyclopentadienyl rings, which are inequivalent in the static structure (Chart 1). This fluxional behavior can be attributed to the fast rotation, on the NMR time scale, of the OCH<sub>3</sub> groups around the O–C(carbyne) bond, and it has been previously studied in detail for other alkoxycarbyne complexes;<sup>10b,20</sup> therefore this was not investigated further.

The bis(alkoxycarbyne) complexes **7** and **8** are isoelectronic and isostructural to the bis(phosphide) complexes **5** and **6**, with a bridging PR<sub>2</sub> group being replaced by a COR ligand (Chart 1). The solid-state structure of complex **7** was confirmed through an X-ray study (see ref 18 and Table 2) and confirms the expected analogies. In particular, the very short intermetallic length of 2.474(1) Å is almost the same as that found for the neutral complex **4** (see ref 17 and Table 2) and is consistent with the triple Mo–Mo bond formulated for these 30-electron cations. However, the nature of the intermetallic interaction in all these unsaturated species will be discussed in detail later on the basis of the DFT calculations carried out on these complexes.

Spectroscopic data for compounds **7** and **8** (Table 1) are essentially consistent with the structure found in the solid state for **7**, but once more they suggest that a dynamic process occurs in solution. The phosphorus nuclei ( $\delta_P$  ca. 264 ppm) exhibit the characteristic highly deshielded NMR resonances found for

other 30-electron dimolybdenum complexes having dialkyl- or diarylphosphide bridges.<sup>9,16–19</sup> However, while the <sup>1</sup>H NMR spectrum of complex **7** would be fully consistent with the C<sub>2</sub> symmetry found in the crystal for that complex, the cation in **8** cannot have this symmetry element; therefore the presence of only one resonance for the inequivalent Cp ligands suggests the occurrence of a dynamic process generating an effective symmetry plane. Actually, a similar process must be operative even for compound **7**, since each of the two inequivalent cyclohexyl groups gives rise to four (instead of six) <sup>13</sup>C NMR resonances. Thus we have to assume again the occurrence of fast rotation (on the NMR time scale) of the alkoxy groups around the corresponding O–C(carbyne) bonds. This process does not affect the carbyne C atoms, which give rise to the characteristic strongly deshielded <sup>13</sup>C NMR resonances (ca. 365 ppm).

**Synthesis and Structural Characterization of New Cationic Hydroxycarbyne Complexes and Their Hydride Isomers.** Just as the neutral complexes **2** and **3** experience an easy O-methylation at their bridging carbonyls, they are protonated at the same position by using HBF<sub>4</sub>·OEt<sub>2</sub>, then giving the corresponding hydroxycarbyne derivatives [Mo<sub>2</sub>Cp<sub>2</sub>( $\mu$ -COH)( $\mu$ -PEt<sub>2</sub>)<sub>2</sub>]BF<sub>4</sub> (**9**) and [Mo<sub>2</sub>Cp<sub>2</sub>( $\mu$ -COH)( $\mu$ -COMe)( $\mu$ -PCy<sub>2</sub>)]BF<sub>4</sub> (**10**), respectively (Chart 2). In contrast to the alkoxycarbyne complexes **5**–**8**, the dichloromethane solutions of the hydroxycarbyne complexes **9** and **10** are thermally unstable, and they rearrange above ca. 273 K (**9**) or 253 K (**10**) to give initially the corresponding hydride-carbonyl isomers [Mo<sub>2</sub>Cp<sub>2</sub>(H)( $\mu$ -PEt<sub>2</sub>)(CO)]BF<sub>4</sub> (**11**) and [Mo<sub>2</sub>Cp<sub>2</sub>(H)( $\mu$ -COMe)( $\mu$ -PCy<sub>2</sub>)(CO)]BF<sub>4</sub> (**12**) in a quite selective way (Chart 2). This rearrangement is unexpected, since the related hydroxycarbyne complexes [Mo<sub>2</sub>Cp<sub>2</sub>( $\mu$ -COH)( $\mu$ -PR<sub>2</sub>)<sub>2</sub>] (M = W, R = Ph;<sup>11</sup> M = Mo, R = Cy<sup>9</sup>) do not experience a similar transformation, but just a slow and generalized decomposition. We can quote, however, a related behavior in the 32-electron complex [W<sub>2</sub>Cp<sub>2</sub>( $\mu$ -COH)( $\mu$ -Ph<sub>2</sub>-PCH<sub>2</sub>PPh<sub>2</sub>)(CO)<sub>2</sub>]BF<sub>4</sub>, which undergoes a rather complex, solvent-assisted transformation into a mixture of the hydride derivatives [W<sub>2</sub>Cp<sub>2</sub>( $\mu$ -H)( $\mu$ -Ph<sub>2</sub>PCH<sub>2</sub>PPh<sub>2</sub>)(CO)<sub>x</sub>]BF<sub>4</sub> (x = 2 and 4).<sup>10b</sup> In any case, the hydrides **11** and **12** are yet unstable species that decompose progressively upon manipulation and therefore could not be isolated as pure solids.

The structural characterization of compounds **9** and **10** can be made easily by comparison of their spectroscopic data (Table 1) with those of the related diphenyl- and dicyclohexylphosphide-bridged analogues [M<sub>2</sub>Cp<sub>2</sub>( $\mu$ -COH)( $\mu$ -PR<sub>2</sub>)<sub>2</sub>]BF<sub>4</sub> (M = W, R = Ph;<sup>11</sup> M = Mo, R = Cy<sup>9</sup>) and with those of the methoxycarbyne compounds **6** and **7**, therefore not needing a detailed discussion. The most relevant data are the appearance of characteristic strongly deshielded resonances in the corresponding <sup>1</sup>H (ca. 13 ppm) and <sup>13</sup>C (ca. 365 ppm) NMR spectra, these clearly denoting the presence of the hydroxycarbyne ligand.

Compounds **11** and **12** are, on the other hand, quite unusual in having their hydride ligands terminally bound to a metal atom involved in a triple intermetallic bond, since 30-electron binuclear complexes usually display bridging hydride ligands.<sup>10b,12,21</sup> In fact, the only reported structural analogue of these compounds is the cationic complex [Mo<sub>2</sub>Cp<sub>2</sub>(H)( $\mu$ -PCy<sub>2</sub>)-

(19) García, G.; García, M. E.; Melón, S.; Riera, V.; Ruiz, M. A.; Villafañe, F. *Organometallics* **1997**, *16*, 624.

(20) For examples of fluxional behavior, see for example: (a) Bavaro, L. M.; Keister, J. B. *J. Organomet. Chem.* **1985**, *287*, 357. (b) Keister, J. B.; Payne, M. W.; Muscatella, M. *J. Organometallics* **1983**, *2*, 219. (c) Johnson, B. F. G.; Lewis, J.; Orpen, A. G.; Raithby, P. R.; Süß, G. *J. Organomet. Chem.* **1979**, *173*, 187. (d) Keister, J. B. *J. Chem. Soc., Chem. Commun.* **1979**, 214. (e) Gavens, P. D.; Mays, M. J. *J. Organomet. Chem.* **1978**, *162*, 389.

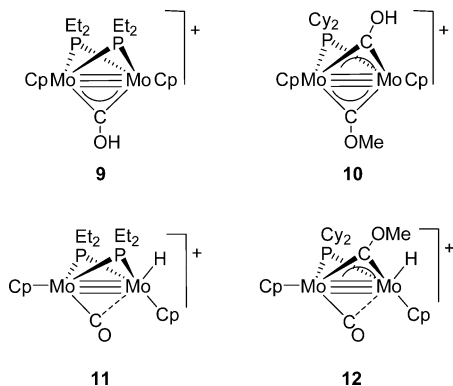
(21) (a) Süß-Fink, G.; Therrien, B. *Organometallics* **2007**, *26*, 766. (b) Alvarez, C. M.; Alvarez, M. A.; García, M. E.; Ramos, A.; Ruiz, M. A.; Lanfranchi, M.; Tiripicchio, A. *Organometallics* **2005**, *24*, 7. (c) Suzuki, H. *Eur. J. Inorg. Chem.* **2002**, 1009. (d) Kang, B. S.; Koelle, U.; Thewalt, U. *Organometallics* **1991**, *10*, 2569. (e) Forrow, W. J.; Knox, S. A. R. *J. Chem. Soc., Chem. Commun.* **1984**, 679. (f) Hoyano, J. K.; Graham, W. A. *G. J. Am. Chem. Soc.* **1982**, *104*, 3722.



**Table 2.** Selected DFT-Optimized Bond Lengths (Å) and Angles (deg)<sup>a</sup>

parameter	2 <sup>b</sup>	6 <sup>c</sup>	A	3 <sup>d</sup>	7 <sup>e</sup>
Mo1–Mo2	2.536 {2.515(2)}	2.537 {2.532(1)}	2.499	2.502 {2.479(2)}	2.501 {2.474(1)}
Mo1–C*		1.998 {1.97(1)}		1.997 {1.974(5)}	2.035 {2.00(1)}
Mo2–C*		2.034 {1.97(1)}		2.026 {2.011(5)}	2.006 {1.99(1)}
Mo1–CO	2.110 {2.08(1)}		2.120 2.089	2.117 {2.091(5)}	
Mo2–CO	2.108 {2.08(1)}		2.091 2.118	2.113 {2.073(6)}	
C*–OMe		1.307 {1.39(1)}		1.324 {1.332(5)}	1.305 {1.31(1)}
C–O	1.193 {1.201}		1.206 1.206	1.193 {1.190(6)}	1.305 {1.33(1)}
O–Me		1.446 {1.40(1)}		1.436 {1.443(6)}	1.449 {1.47(2)}
Mo–P	2.415 {2.374(3)}	2.433 {2.372(3)}	2.437	2.445 {2.392(2)}	2.466 {2.405(3)}
	2.409 {2.389(3)}	2.423 {2.372(3)}	2.439	2.450 {2.395(2)}	2.469 {2.409(3)}
	2.409 {2.373(3)}	2.428 {2.372(3)}			
	2.416 {2.384(3)}	2.437 {2.372(3)}			
C–O–Me		120.5 {114(1)}		118.4 {118.2(4)}	120.0 {116(1)}
					119.9 {117(1)}

<sup>a</sup> Experimental values, as derived from X-ray data for the same or related species, in brackets; the Mo1 label corresponds to the metal atom positioned away from the methyl group of the methoxycarbonyl ligand, except for compounds **2**, **A**, and **7**, for which both metal centers are equivalent; C\* refers to the bridgehead atom of the carbonyl ligand. <sup>b</sup> Experimental values for [Mo<sub>2</sub>Cp<sub>2</sub>(μ-PPH<sub>2</sub>)<sub>2</sub>(μ-CO)] (see ref 50). <sup>c</sup> Experimental values for the cation in [W<sub>2</sub>Cp<sub>2</sub>(μ-COMe)(μ-PPH<sub>2</sub>)<sub>2</sub>](CF<sub>3</sub>SO<sub>3</sub>) (see ref 11). <sup>d</sup> Experimental values for the ethoxycarbonyl complex **4** (see ref 17). <sup>e</sup> Experimental values for the cation in [Mo<sub>2</sub>Cp<sub>2</sub>(μ-COMe)<sub>2</sub>(μ-PCy<sub>2</sub>)]BF<sub>4</sub> (see ref 18).

**Chart 2**

(CO)]BF<sub>4</sub>, whose structure was confirmed through an X-ray study. This complex could be prepared recently in our laboratory by UV–visible irradiation of dichloromethane solutions of a mixture of the dicarbonyl tautomers [Mo<sub>2</sub>Cp<sub>2</sub>(μ-PCy<sub>2</sub>)(μ-κ<sup>2</sup>-HPCy<sub>2</sub>)(CO)<sub>2</sub>]]BF<sub>4</sub> and [Mo<sub>2</sub>Cp<sub>2</sub>(μ-H)(μ-PCy<sub>2</sub>)(CO)<sub>2</sub>]]BF<sub>4</sub>.<sup>9</sup> Interestingly, this hydride complex cannot be formed via thermal or photochemical rearrangement of the corresponding hydroxycarbonyl isomer [Mo<sub>2</sub>Cp<sub>2</sub>(μ-COH)(μ-PCy<sub>2</sub>)]BF<sub>4</sub>.

Spectroscopic data in solution for **11** (Table 1 and Experimental Section) are in general agreement with those previously reported for [Mo<sub>2</sub>Cp<sub>2</sub>(H)(μ-PCy<sub>2</sub>)(CO)]BF<sub>4</sub>.<sup>9</sup> For example, the phosphorus nuclei give rise to a similar <sup>31</sup>P NMR resonance [285.4 vs 305.2 ppm for the μ-PCy<sub>2</sub> analogue], which is even more deshielded than those of 30-electron phosphide-bridged dimolybdenum complexes having three bridging ligands, such as the complexes **1**–**10**. The presence of a terminal hydride in **11** is denoted by the appearance of a poorly shielded hydride resonance [ $\delta_{\text{H}} = -1.47$  vs  $-1.60$  ppm for the μ-PCy<sub>2</sub> analogue], to be compared with the more shielded resonances characteristic of bridging hydrides, such as those in the electron-precise tetracarbonyls [M<sub>2</sub>Cp<sub>2</sub>(μ-H)(μ-PR<sub>2</sub>)(CO)<sub>4</sub>] (M = Mo, W; R = Cy, Et, Ph) (ca.  $-15$  ppm).<sup>16</sup> Moreover, the hydride shielding in **11** is still considerably lower than that observed in the isoelectronic hydride-bridged complex [Mo<sub>2</sub>Cp<sub>2</sub>(μ-H)(μ-PCy<sub>2</sub>)(CO)<sub>2</sub>], also having a triple intermetallic bond ( $\delta_{\text{H}} = -6.94$

ppm).<sup>17,21b</sup> On the other hand, the proposal of a semibridging character for the carbonyl ligand in **11** follows from its relatively low C–O stretching frequency (1843 cm<sup>-1</sup>) and high <sup>13</sup>C chemical shift ( $\delta_{\text{C}} = 259.8$  ppm). We note that the related complex [Mo<sub>2</sub>Cp<sub>2</sub>(H)(μ-PCy<sub>2</sub>)(CO)]BF<sub>4</sub> displays a semibridging carbonyl in the solid state and exhibits similar IR and <sup>13</sup>C NMR features in solution ( $\nu_{\text{CO}} = 1838$  cm<sup>-1</sup>,  $\delta_{\text{C}} = 260.6$  ppm).<sup>9</sup>

Complex **11** exhibits fluxional behavior in solution, as deduced from the appearance of single <sup>1</sup>H or <sup>13</sup>C NMR resonances for the inequivalent Cp ligands and from the equivalence of the diastereotopic <sup>13</sup>C cyclohexyl resonances. A similar behavior was found for the complex [Mo<sub>2</sub>Cp<sub>2</sub>(H)(μ-PCy<sub>2</sub>)(CO)]BF<sub>4</sub> and was explained by assuming the occurrence of a concerted scrambling of the CO and H ligands between both metal atoms, this effectively generating the required symmetry plane relating both metal centers.<sup>9</sup> This seems to be the case also for compound **11**. Indeed, on lowering the temperature, its hydride resonance remains unchanged, but the cyclopentadienyl <sup>1</sup>H NMR resonance at 5.75 ppm first broadens and then eventually splits into two well-separated resonances ( $\delta_{\text{H}} = 5.83$  and 5.73 ppm at 213 K), in agreement with the rigid structure shown in Chart 2. From the corresponding coalescence temperature (ca. 250 K) we can estimate for the corresponding fluxional process an activation barrier of ca. 52–(±1) kJ mol<sup>-1</sup>,<sup>22</sup> to be compared with a barrier of 43(±1) kJ mol<sup>-1</sup> calculated for [Mo<sub>2</sub>Cp<sub>2</sub>(H)(μ-PCy<sub>2</sub>)(CO)]BF<sub>4</sub>.<sup>9</sup> This difference can be explained by assuming that the lower steric demands of the PEt<sub>2</sub> bridges (compared to PCy<sub>2</sub> bridges), would allow for a higher stabilization of the ground-state structure (puckered Mo<sub>2</sub>P<sub>2</sub> central framework, with closer mutual approach of substituents on different P atoms) relative to the transition state (flat Mo<sub>2</sub>P<sub>2</sub> framework).

The spectroscopic data for compound **12** (Table 1 and Experimental Section) are very similar to those just discussed for **11**, and they need not be analyzed in detail. Thus, the structures for these hydride complexes are assumed to be essentially identical, by just replacing one of the phosphide groups by the isoelectronic methoxycarbonyl ligand. The latter is expected to be a poorer  $\sigma$ -donor and better  $\pi$ -acceptor ligand

than a dialkylphosphide ligand, which is consistent with the observed C–O stretching frequency for **12** ( $1873\text{ cm}^{-1}$ ), some  $35\text{ cm}^{-1}$  above that of **11**. Interestingly, complex **12** also exhibits fluxional behavior in solution, presumably also involving a concerted scrambling of the CO and H ligands between both metals. From the corresponding coalescence temperature of the  $^1\text{H}$  NMR cyclopentadienyl resonances (ca.  $263\text{ K}$ ) we can estimate an activation barrier of ca.  $55(\pm 1)\text{ kJ mol}^{-1}$ ,<sup>22</sup> only marginally above that calculated for **11**.

**Computational Studies.** Thanks to the rapid progress in computing power and the development of new methodologies, quantum mechanical calculations for transition metal complexes are today accessible for much more complex systems. In particular, the great computational efficiency and chemical accuracy of the DFT methods allow the study of real (rather than model) molecules of the size of the binuclear metal complexes discussed here.<sup>23</sup>

We have carried out DFT calculations (see Experimental Section for further details) for the new cationic methoxycarbyne complexes  $[\text{Mo}_2\text{Cp}_2(\mu\text{-COMe})(\mu\text{-PEt}_2)_2]^+$  (**6**) and  $[\text{Mo}_2\text{Cp}_2(\mu\text{-COMe})_2(\mu\text{-PCy}_2)]^+$  (**7**), as well as for their carbonyl-bridged precursors  $[\text{Mo}_2\text{Cp}_2(\mu\text{-PEt}_2)_2(\mu\text{-CO})]$  (**2**),  $[\text{Mo}_2\text{Cp}_2(\mu\text{-PCy}_2)(\mu\text{-CO})_2]^-$  (**A**), and  $[\text{Mo}_2\text{Cp}_2(\mu\text{-COMe})(\mu\text{-PCy}_2)(\mu\text{-CO})]$  (**3**). This will allow us to better understand not only the metal–metal and metal–carbon bonding in these unsaturated complexes but also the electronic changes accompanying the process of methylation at the oxygen atom of a bridging carbonyl ligand. All these complexes exhibit a face-sharing bioctahedral structure (assuming the Cp groups as equivalent to three terminal ligands) and have a total of 30 electrons for metal binding, this leading to the formulation of a triple metal–metal bond, according to the EAN rule. First, we will discuss the optimized geometries calculated for these molecules. This will be followed by an analysis of the electronic structure and bonding in these unsaturated complexes from two distinct points of view: the properties of the relevant molecular orbitals and the topological properties of the electron density as managed in the AIM theory.<sup>24</sup>

**Optimized Geometries.** The most relevant parameters derived from the geometry optimization of the anion  $[\text{Mo}_2\text{Cp}_2(\mu\text{-PCy}_2)(\mu\text{-CO})_2]^-$  (**A**), the cations in **6** and **7**, and the neutral compounds **2** and **3** can be found in Table 2, with the corresponding views being collected in Figure 1. The experimental data (from X-ray diffraction studies) for the same or closely related species are also collected in that table. As it can be seen from inspection of all these data, the optimized bond lengths are in quite good agreement with the corresponding experimental data, although those involving the metal atoms tend to be slightly greater (less than  $0.05\text{ \AA}$ ) than the corresponding values measured in the solid state for the same or strongly comparable compounds by X-ray diffraction. This is a common tendency with the functionals currently used in the DFT computations of transition metal compounds.<sup>12,23a,25</sup>

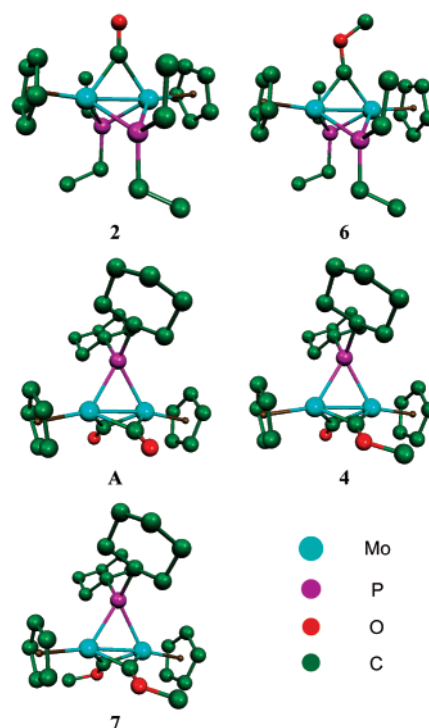


**Figure 1.** Optimized geometries for complexes **2**, **6**, **A**, **3**, and **7**, with hydrogen atoms omitted for clarity.

The intermetallic distances are all found within the range  $2.499\text{--}2.537\text{ \AA}$  and are almost unaffected by the methylation at the carbonyl bridges, with changes being on the order of just  $0.001\text{ \AA}$ . The nature of the donor atoms at the bridging positions is more relevant in this respect: as expected, complexes with one P-donor and two C-donor bridging ligands exhibit distances shorter (by ca.  $0.035\text{ \AA}$ ) than those complexes with one C-donor and two P-donor bridges, doubtless as a consequence of the lower covalent radius of carbon when compared to that of phosphorus.

The Mo–C bond lengths follow also the expected trends, with the Mo–C(carbonyl) lengths (ca.  $2.10\text{ \AA}$ ) longer than the Mo–C(carbyne) distances (ca.  $2.01\text{ \AA}$ ), in agreement with the change in the formal order of the corresponding bonds, which increase from 1 in the bridging carbonyls to 1.5 in the bridging methoxycarbyne ligands. The latter exhibit a slightly asymmetric coordination, being closer to the metal center placed away from the methyl group (Mo1 in Table 2), which is possibly a genuine steric effect. We note finally the excellent fit of the calculated C–O lengths and C–O–C angles with the corresponding experimental data, with the larger deviation in the case of **6** being considered as not significant, due to the low quality of the experimental data available, with a disorder in the methoxycarbyne ligand.<sup>11</sup>

Frequency analysis was carried out in all the stationary points to ensure that the optimized geometries correspond to global minima of the potential energy surface (PES). For all complexes but **6** and **7** this analysis showed no imaginary frequencies, this allowing us to classify the corresponding geometries as real minima in the PES. For the cations in **6** and **7**, however, the geometry optimization converged with one imaginary vibrational frequency of low value (ca.  $10i\text{ cm}^{-1}$ ), which we attribute to the internal rotation of one of the cyclopentadienyl ligands. We thus concluded that there is a genuine minimum of energy identical to or very close to the stationary point in question regarding the geometry of the  $\text{Mo}_2\text{P}_x\text{C}_y$  core, and therefore we

(22) Calculated using the modified Eyring equation  $\Delta G^\ddagger = 19.14T_c[9.97 + \log(T_c/\Delta\nu)]$  ( $\text{J mol}^{-1}$ ). See: Günther, H. *NMR Spectroscopy*; John Wiley: Chichester, UK, 1980; p 243.

(23) (a) Koch, W.; Holthausen, M. C. *A Chemist's Guide to Density Functional Theory*, 2nd ed.; Wiley-VCH: Weinheim, 2002. (b) Ziegler, T. *Chem. Rev.* **1991**, *91*, 651. (c) Foresman, J. B.; Frisch, A. E. *Exploring Chemistry with Electronic Structure Methods*, 2nd ed.; Gaussian, Inc.: Pittsburgh, 1996.

(24) (a) Bader, R. F. W. *Atoms in Molecules—A Quantum Theory*; Oxford University Press: Oxford, 1990. (b) Bader, R. F. W. *Chem. Rev.* **1991**, *91*, 893.

(25) Cramer, C. J. *Essentials of Computational Chemistry*, 2nd ed.; Wiley: Chichester, UK, 2004.

**Table 3. Calculated and Experimental C–O Stretching Frequencies<sup>a</sup>**

compd	$\nu_{\text{st}}(\text{C–O})/\text{cm}^{-1}$		
	calcd <sup>b</sup>	expt <sup>c</sup>	% <sup>d</sup>
<b>A</b>	1770(34)	1643(m, sh)	7.7
	1756(100)	1624(vs)	8.1
<b>2</b>	1826	1697	7.6
<b>3</b>	1829 <sup>e</sup>	1700 <sup>e</sup>	7.6
	1315		
<b>6</b>	1349	1271 <sup>f</sup>	6.1
<b>7</b>	1367	1308 <sup>f</sup>	4.5
	1347	1273 <sup>f</sup>	5.8

<sup>a</sup> Values corresponding to the CO or COME ligands, with relative intensities in brackets; experimental data for complexes **A**, **2**, and **3** taken from refs 16 and 17. <sup>b</sup> Uncorrected. <sup>c</sup> In THF solution, unless otherwise stated. <sup>d</sup> (calcd – expt)/expt. <sup>e</sup> Carbonyl ligand. <sup>f</sup> Recorded in Nujol mull.

did not follow any further the imaginary eigenvector in search of a stationary point with no imaginary vibrational frequencies.

The calculated and experimental values of the C–O stretching frequencies for both the carbonyl and the methoxycarbyne ligands in these complexes are shown in Table 3. As it can be appreciated, the calculated values overestimate the experimental figures by roughly 7%, which is a normal bias for DFT-derived IR stretching frequencies.<sup>26</sup> In any case, the calculated values for the methoxycarbyne complexes allow us to unambiguously assign the experimental IR bands. Bearing in mind that for simple molecules such as organic ethers the C–O stretching frequencies tend to appear in the range 1150–1250 cm<sup>-1</sup>, even when including sp<sup>2</sup>-hybridized carbon atoms, the high values measured for our methoxycarbyne complexes, ca. 1290 cm<sup>-1</sup>, might be considered as indicative of the persistency of a significant  $\pi$ -bonding interaction at the C–OMe bond, also consistent with the conformation of the ligand (arrangement in the Mo<sub>2</sub>C plane and C–O–C angles close to 120°). As it will be discussed later on, this kind of interaction is fully consistent with the MO and AIM analysis of the bonding in these methoxycarbyne complexes.

The electronic charges calculated for the different complexes are shown in Table S1 (see Supporting Information), which includes the Mulliken charges,<sup>27</sup> as well as those derived from the NBO analysis (NPA charges).<sup>28</sup> The complexes having bridging carbonyls (**2**, **A**, and **3**) display the highest negative atomic charges at the corresponding oxygen atoms, in agreement with the preferential addition of the hard cations Me<sup>+</sup> or H<sup>+</sup> at this site. Since the high-energy occupied molecular orbitals of the carbonyl complexes do not involve their oxygen atoms (see below), then we can conclude that the formation of the hydroxy- and methoxycarbyne complexes discussed in this paper are essentially charge-controlled reactions. Upon formation of the methoxycarbyne ligands, the atomic charges indicate a decrease of electron density at the Mo atoms and a significant increase of ca. 0.16e at the C(carbyne) atoms, with charges of ca. –0.02e (Mulliken) or +0.26e (NPA), to be compared with the values of ca. +0.14e (Mulliken) or +0.42e (NPA) in the carbonyl-bridged precursors. Incidentally, we note that low atomic charges were also found for the C(carbyne) atom after the semiempirical

(26) Yu, L.; Srinivas, G. N.; Schwartz, M. J. *Mol. Struct. (THEOCHEM)* **2003**, 625, 215.

(27) Mulliken, R. S. *J. Chem. Phys.* **1955**, 23, 1833.

(28) Mulliken population analyses fail to give a useful and reliable characterization of the charge distribution in many cases, especially when highly ionic compounds and diffuse basis functions are involved. Charges calculated according to the natural population analysis (NPA) do not show these deficiencies and are more independent of the basis set: (a) Reed, A. E.; Weinstock, R. B.; Weinhold, F. *J. Chem. Phys.* **1985**, 83, 735. (b) Reed, A. E.; Curtis, L. A.; Weinhold, F. *Chem. Rev.* **1988**, 88, 899.

MO calculations carried out on the cluster [Co<sub>3</sub>( $\mu_3$ -COMe)-(CO)<sub>9</sub>].<sup>15</sup> In any case, however, the highest positive charges for all these complexes are located at the phosphorus atoms, in agreement with the good electron-donor properties of the PR<sub>2</sub> ligands, while the highest negative charges are still located at the oxygen atoms.

**MO Analysis.** Molecular orbital theory is the most widely used tool for studying the chemical bond in molecules.<sup>25,29</sup> In the DFT-based framework, Kohn–Sham (KS) orbitals, when compared to classical MOs, are not only associated with the one-electron potential which includes all nonclassical effects but are also consistent with the exact ground-state density. Moreover, the power of the KS orbitals has been recognized by many authors as being similar to that of the classical MOs for the analysis of chemical bonding, at least in a qualitative way.<sup>25,30</sup> Accordingly, a detailed analysis of the corresponding KS orbitals has been performed to obtain information about the bonding in our unsaturated molecules.

The electronic structure of face-sharing bioctahedral complexes has received considerable attention from computational chemists, which, however, have been mainly concerned with non-organometallic compounds.<sup>31</sup> The metal–metal bonding in these systems follows from the occupation of one  $\sigma$ - and two  $\delta$ -bonding MOs. Using this scheme as a first approach, we can therefore expect an occupation up to the  $\delta$ -bonding orbitals ( $\sigma^2\delta^4$ ) for our 30-electron organometallic complexes, and thus formally a triple metal–metal bond.<sup>12,32</sup> This situation, however, can be much more complicated in our complexes, since in low-symmetry systems a mixture between  $\delta$ -bonding orbitals and high-energy  $\pi$  counterparts (from the metals or the bridging ligands present there) can occur to yield more complicated bonding patterns. With this in mind, we will first analyze the molecular orbitals of the bis(diethylphosphide) complexes **2** and **6** and then those of the dicyclohexylphosphide complexes **A**, **3**, and **7**. The first couple illustrates the effect of a single methylation at a bridging carbonyl, while the latter triad corresponds to two successive methylation steps and allows an internal comparison between carbonyl and bridging methoxycarbyne ligands.

**Molecular Orbitals of Compounds 2 and 6.** The most relevant orbitals of compounds **2** and **6** are depicted in Figure 2, with their associated energy and prevalent bonding character. The highest occupied molecular orbital (HOMO, MO 95) of the monocarbonylic complex **2** corresponds essentially to one of the two components of the metal–carbonyl  $\sigma$  bond, involving metal d orbitals. This is quite surprising since for these highly unsaturated complexes we should expect the HOMO to be a metal–metal bonding  $\delta$  orbital, as noted above. Indeed the next three orbitals are those accounting for the metal–metal bonding: two of them can be clearly identified as the  $\sigma$  (MO 92) and one of the  $\delta$  (MO 94) components of the expected triple metal–metal bond.<sup>33</sup> However, the second  $\delta$  component of the triple bond (MO 93) shows an important participation of the

(29) (a) Jean, Y. *Molecular Orbitals of Transition Metal Complexes*; Oxford University Press: Oxford, UK, 2005. (b) Jean, Y.; Volatron, F.; Burdett, J. *An Introduction to Molecular Orbitals*; Oxford University Press: Oxford, UK, 1993.

(30) See, for example: (a) Kohn, W.; Becke, A. D.; Parr, R. G. *J. Phys. Chem.* **1996**, 100, 12974. (b) Baerends, E. J.; Gritsenko, O. V. *J. Phys. Chem. A* **1997**, 101, 5383. (c) Stowasser, R.; Hoffmann, R. *J. Am. Chem. Soc.* **1999**, 121, 3414. (d) Baerends, E. J. *Theor. Chem. Acc.* **2000**, 103, 265.

(31) Petrie, S.; Stranger, R. *Inorg. Chem.* **2003**, 42, 4417, and references therein.

(32) (a) Collman, J. P.; Boulatov, R. *Angew. Chem., Int. Ed.* **2002**, 41, 3948. (b) Summerville, R. H.; Hoffmann, R. *J. Am. Chem. Soc.* **1979**, 101, 3821.



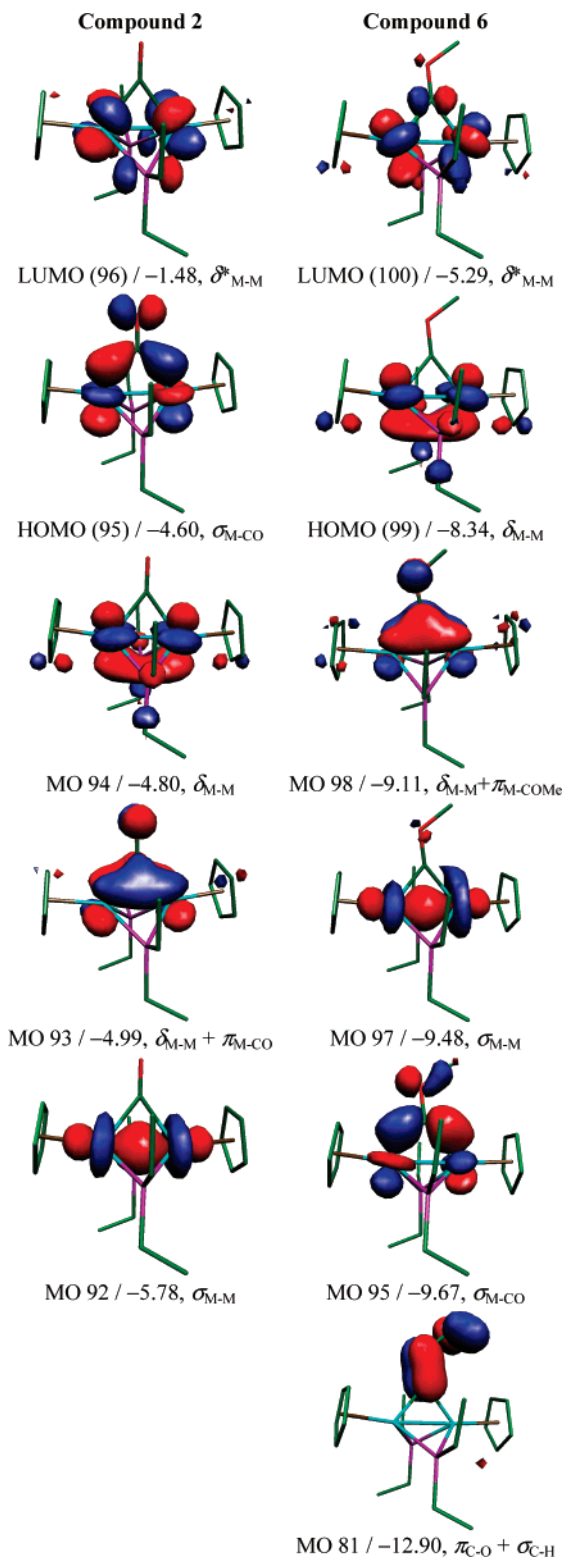


**Figure 2.** Selected molecular orbitals of complexes **2** and **6**, with their energies and main bonding character indicated below.

$\pi^*_{C-O}$  orbital of the bridging carbonyl and, therefore, implies the presence of significant metal-to-carbonyl  $\pi$  back-bonding. The corresponding electrons are thus substantially delocalized over the  $Mo_2C$  triangle, in detriment of the direct metal–metal bonding. A similar effect was previously reported by Hoffman

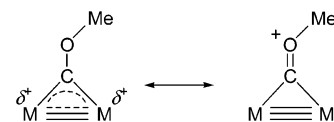


**Figure 3.** Canonical forms used to describe the bonding in methoxycarbyne complexes.

and co-workers for the complexes  $[M_2Cp_2(CO)_4]$  ( $M = Cr, Mo, W$ ), in which the transition of the carbonyl ligands from terminal to semibridging was calculated to cause a decrease in the intermetallic  $\pi$ -bonding interaction.<sup>34</sup> In summary, we can describe the intermetallic interaction in complex **2** as a triple metal–metal bond somewhat weakened due to back-bonding ( $\delta_{MM}$  to  $\pi^*_{CO}$ ) to the bridging carbonyl.

As for the methoxycarbyne complex **6**, the frontier MOs are similar to those of its precursor **2**, except for some significant differences. The most striking effect of the incorporation of the methyl group is the stronger stabilization (compared to that of the other frontier MOs) of the frontier  $\sigma_{M-C}$  orbital (the HOMO in **2**), now appearing as MO 95, below the three orbitals accounting for the intermetallic interaction. The latter includes the HOMO of the molecule (MO 99), now corresponding to one of the two  $\delta$  components of the triple metal–metal bond. This is followed by the  $\delta$  orbital originally involved in the  $\pi$  back-bonding to the CO bridge, now exhibiting a more pronounced delocalization over the  $Mo_2C$  triangle (MO 98), and then by the  $\sigma$ -bonding orbital (MO 97). The orbital MO 98 therefore retains significant metal–metal  $\delta$ -bonding character while becoming the  $\pi$  component of the metal–carbyne bond (the two  $\sigma$  components of that bond are described by MO 95 and the low-energy orbital MO 57). As concerning the bonding within the methoxycarbyne ligand, the nature of MO 81 indicates the persistence of significant  $\pi$ -bonding interaction in the C–O bond of this ligand (a neat  $\pi$  bond in the carbonyl precursor). This interaction must compete necessarily with the  $\pi_{MC}$ -bonding interaction implied by MO 98, since both molecular orbitals share the same atomic orbital of the carbon atom. Thus a stronger  $\pi$ -bonding interaction between the C(carbyne) and O atoms must imply a weaker Mo–C  $\pi$ -bonding interaction and vice versa. This description parallels the two canonical forms traditionally proposed to explain the metal–alkoxycarbyne bond in binuclear complexes, which imply partial double-bond character in both the M–C and C–O bonds (Figure 3). The retention of a significant (but only partial)  $\pi$ -bonding interaction between the C and O atoms explains the short values (ca. 1.30 Å, Table 2) of the corresponding C–O bonds in these systems, with figures somewhat shorter than those found for comparable single bonds, such as the  $C(sp^2)$ –O bonds of organic molecules (ca. 1.35 Å), but still far from the reference values for double C–O bonds (ca. 1.21 Å).<sup>35</sup> In summary, we can describe the intermetallic interaction in complex **6** also as a triple metal–metal bond, but significantly weakened now due to  $\pi$  bonding to the bridgehead carbon atom of the carbyne ligand, which in turn is partially involved in a  $\pi$ -bonding interaction with its oxygen atom.

We note finally that the lowest unoccupied molecular orbitals (LUMO) of compounds **2** and **6** are largely metal-based molecular orbitals and exhibit  $\delta^*_{M-M}$ -antibonding character. These orbitals are relevant to the understanding of the reactivity of these compounds and lead us to the prediction that the

(33) The characterization of these orbitals as  $\sigma$ ,  $\pi$ , or  $\delta$  bonding is arbitrary to some extent, but nevertheless it is a useful distinction based on the predominant type of orbital overlap.

(34) Jennis, E. D.; Pinhas, A. R.; Hoffmann, R. *J. Am. Chem. Soc.* **1980**, *102*, 2576.

(35) Allen, F. H.; Kennard, O.; Watson, D. G.; Brammer, L.; Orpen, G.; Taylor, R. *J. Chem. Soc., Perkin Trans. 2* **1987**, S1.

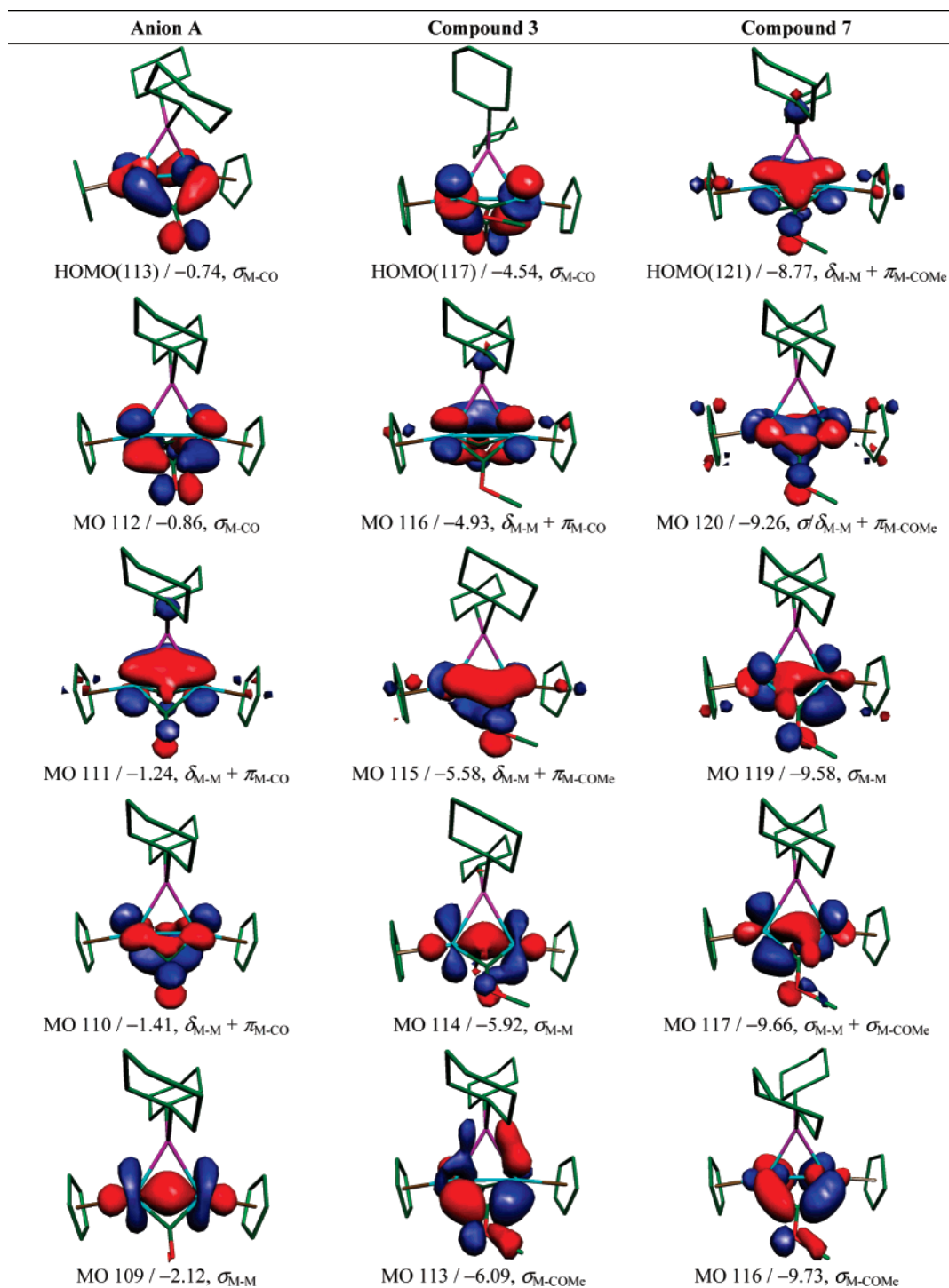


**Figure 4.** Selected molecular orbitals of complexes A, 3, and 7, with their energies and main bonding character indicated below.

incorporation of electron-donor ligands to the dinuclear center under orbital-controlled conditions is accompanied by a reduction of the intermetallic bond order, as expected for such highly unsaturated compounds.

**Molecular Orbitals of Compounds A, 3, and 7.** The relevant orbitals for the anion  $[\text{Mo}_2\text{Cp}_2(\mu\text{-PCy}_2)(\mu\text{-CO})_2]^-$  (A) and its methoxycarbonyl derivatives 3 and 7 are collected in Figure 4, and an orbital correlation diagram is shown in Figure 5. The general trends in these complexes are similar to those previously discussed for compounds 2 and 6. The successive methylation at the oxygen atoms of the carbonyl ligands causes again a strong and progressive stabilization of the (now two) frontier MOs having  $\sigma$  metal-carbon bonding character. The triple

intermetallic bond in these complexes is also made up of a  $\sigma$  and two  $\delta$  components, but now only the  $\sigma$  component [MO 109 (A), 114 (3), and 117 (7)] has pure metal character (in complex 7 this orbital even appears somewhat mixed with a  $\sigma_{MC}$ -bonding orbital, MO 119). The  $\delta$  components of this bond are mixed with the appropriate carbon orbitals, thus implying the presence of significant  $\pi$  back-bonding to the carbonyls (A),  $\pi$  bonding with the methoxycarbonyls (7), or a mixture of both tricentric interactions (3), all of them a detriment to the direct intermetallic bond. As for the bonding within the methoxycarbonyl ligand, the situation is identical to that described for complex 6, so that low-energy orbitals representing a partial



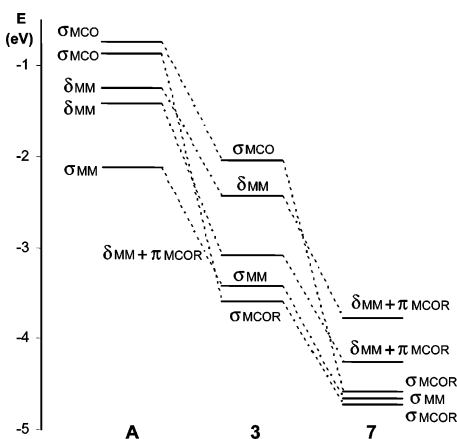


**Figure 5.** Correlation diagram of the frontier molecular orbitals of complexes **A**, **3**, and **7**. Those of compounds **3** and **7** are represented 2.5 and 5.0 eV above their actual energy, respectively.

$\pi_{CO}$ -bonding interaction for each of these ligands are found for both **3** and **7** (see Supporting Information).

**Topological Analysis of the Electron Density.** The quantum theory of atoms in molecules provides an alternative way of analyzing the chemical bond by inspection of the topology of the total electron density of a molecule.<sup>24</sup> We have collected in Table 4 the values of the electron density ( $\rho$ ) and its Laplacian  $\nabla^2\rho$  at several bond critical points (bcp) of complexes **2** to **7**. Figure 6 shows electron density maps of the planes M–C(O)–M and M–C(OMe)–M in complex **3**, which are quite representative of the density maps for all other complexes in the planes involving the bridging carbonyl and carbyne ligands.

The first point of interest is the localization of the corresponding bcp for the metal–metal bond in all cases. This is not granted in dinuclear complexes of transition metals having bridging ligands with  $\pi$ -bonding ability such as  $\mu$ -CO or  $\mu$ -CR; for example the intermetallic bcp could not be localized for the singly bonded complexes  $[\text{Fe}_2(\text{CO})_9]$ <sup>36</sup> or  $[\text{Co}_2(\text{CO})_8]$ .<sup>14c</sup> To gain a better understanding of the values of  $\rho$  obtained at the intermetallic bcp's obtained for our complexes, we carried out DFT computations, using the same functional and basis, on some prototype complexes having no bridging ligands that could contribute to the delocalization of the metal–metal interaction (Table 5). We also computed the triply bonded  $[\text{Mo}_2\text{Cp}_2(\text{CO})_4]$ , a representative example of the unsaturated cyclopentadienyl complexes displaying semibridging carbonyls along a formally triple intermetallic bond.<sup>37</sup> As expected, the reduction of the formal metal–metal bond order is accompanied by a strong decrease of the electronic density at the intermetallic bcp for the model compounds. The values of  $\rho$  at the intermetallic bcp in our complexes (ca.  $0.60 \text{ e } \text{\AA}^{-3}$ ) are lower than those calculated for the triply bonded complexes  $[\text{Mo}_2\text{X}_6]$  (ca.  $0.98 \text{ e } \text{\AA}^{-3}$ ), which is not surprising in view of the much shorter intermetallic lengths in the latter complexes and the absence of bridging ligands. Clearly, the presence in compounds **2** to **7** of bridging carbonyl or carbyne ligands involved in  $\pi$ -bonding interactions with the  $\delta$ -bonding orbitals of the metals has the effect of subtracting electronic density from the intermetallic vector and, thus, causes a lowering of the values of  $\rho$  at the bcp. Yet, the figures for compounds **2** to **7** are much higher than those calculated for singly bonded complexes having no carbonyl bridges such as  $[\text{Mo}_2\text{Cp}_2(\text{CO})_6]$  and  $[\text{Mo}_2(\text{CO})_{10}]^{2-}$  (ca.  $0.15 \text{ e } \text{\AA}^{-3}$ , Table 5). Most interestingly, the intermetallic  $\rho$  values for compounds **2**

to **7** are comparable to (even slightly higher than) the figure calculated for the triply bonded  $[\text{Mo}_2\text{Cp}_2(\text{CO})_4]$  ( $0.576 \text{ e } \text{\AA}^{-3}$ ), which exhibits linear semibridging carbonyls. A further observation of interest is that the intermetallic  $\rho$  is only marginally reduced (by ca.  $0.005 \text{ e } \text{\AA}^{-3}$ ) upon formation of the carbyne ligands via methylation of the carbonyl bridges. Thus, it is tempting to conclude that the extent of the  $\pi$  interactions with either the carbonyl or methoxycarbyne bridges in compounds **2** to **7** might be comparable, but perhaps this is just a reflection of the very low contribution of the implied bonding electrons to the total electron density at the intermetallic bcp, due to their tricentric distribution.

The values of  $\nabla^2\rho$  at the intermetallic bcp for our complexes are moderately positive ( $1.90$ – $2.92 \text{ e } \text{\AA}^{-5}$ ), a feature that seems to be a characteristic of metal–metal interactions in transition metal complexes,<sup>38</sup> attributed to the diffuse character of the electrons involved in the bonding.<sup>39</sup> These values are similar to that calculated for  $[\text{Mo}_2\text{Cp}_2(\text{CO})_4]$ , but significantly lower than those for the triply bonded complexes  $[\text{Mo}_2\text{X}_6]$  in Table 5. This is surely just a consequence of the higher internuclear distance for the 30-electron cyclopentadienyl complexes, this implying by force a smoother change of the electronic density along the intermetallic vector.

As for the M–C bonds within the carbonyl and methoxycarbyne ligands, the AIM analysis is fully consistent with the geometric features and orbital analysis discussed above. As expected, the values of  $\rho$  at the M–C bcp's are significantly higher for the M–C(carbyne) bonds (in the range  $0.83$  to  $0.93 \text{ e } \text{\AA}^{-3}$ ) than for the M–C(carbonyl) bonds (ca.  $0.71 \text{ e } \text{\AA}^{-3}$ ). We note that the latter figure is comparable to the values reported for the bridging carbonyls at  $[\text{Co}_2(\text{CO})_8]$ ,<sup>39</sup> but we are not aware of any previous topological analysis reported for a carbyne-bridged complex that could be used for comparative purposes. Even so, by taking into account that the progressive increase (from 1 to 3) of the formal M–C bond order in the series  $\text{CrCH}_3/\text{CrCH}_2/\text{CrCH}$  is reflected in a rather modest increase of  $\rho$  at the corresponding Cr–C bcp's ( $0.769$ ,  $0.904$ , and  $1.174 \text{ e } \text{\AA}^{-3}$ , respectively),<sup>40</sup> then we conclude that the average value of  $\rho$  of ca.  $0.88 \text{ e } \text{\AA}^{-3}$  in our complexes is consistent with a substantial multiplicity of the corresponding Mo–C(carbyne) bonds. We note also the disappearance of the minimum of the electron density in the center of the M–C–M triangle involving the methoxycarbyne ligand (right in Figure 6) compared to the analogous plane containing a carbonyl ligand (left in Figure 6), this reflecting the accumulation of  $\pi$ -electron density in this triangle upon methylation of the bridging carbonyls. Finally, the presence of the methoxyl group in the same plane containing the metal and carbyne atoms causes an asymmetry in the coordination of the methoxycarbyne ligand, as already discussed. This causes the electron density at the bcp of the shorter bond to be higher (ca.  $0.90 \text{ e } \text{\AA}^{-3}$ ) than the corresponding value of the longer bond (ca.  $0.83 \text{ e } \text{\AA}^{-3}$ ), as expected.

As for the C–O bond within the methoxycarbyne ligand, we find that the electron density at the corresponding bcp (ca.  $2.10 \text{ e } \text{\AA}^{-3}$ ) has a value intermediate between those at the single C–O bond of the methoxyl group (ca.  $1.58 \text{ e } \text{\AA}^{-3}$ ) and those at the double C–O bond of the carbonyl bridges (ca.  $2.75 \text{ e } \text{\AA}^{-3}$ ). This can be taken as independent evidence for the presence of

(38) Gervasio, G.; Bianchi, R.; Marabello, D. *Chem. Phys. Lett.* **2004**, 387, 481, and references therein.

(39) Macchi, P.; Sironi, A. *Coord. Chem. Rev.* **2003**, 238–239, 383.

(40) Vidal, I.; Melchor, S.; Dobado, J. A. *J. Phys. Chem.* **2005**, 109, 7500.

(36) Bo, C.; Sarasa, J. P.; Poblet, J. M. *J. Phys. Chem.* **1993**, 97, 6362.

(37) Winter, M. J. *Adv. Organomet. Chem.* **1989**, 29, 101.

Table 4. Topological Properties of the Electron Density at the Bond Critical Points<sup>a</sup>

bond	2		6		A		3		7	
	r	$\nabla^2\rho$	r	$\nabla^2\rho$	r	$\nabla^2\rho$	r	$\nabla^2\rho$	r	$\nabla^2\rho$
Mo1–Mo2	0.588	1.90	0.584	2.14	0.615	2.38	0.609	2.52	0.606	2.72
Mo1–C*			0.935	6.08			0.925	6.65	0.920	6.21
									0.831	6.90
Mo2–C*			0.832	6.75			0.835	7.29	0.920	6.20
									0.832	6.90
C*–OMe			2.116	1.42			2.027	0.81	2.128	1.87
									2.129	1.89
O–Me			1.562	–8.21			1.637	–10.38	1.553	–8.19
									1.554	–8.19
Mo1–CO	0.711	5.56			0.698	5.58	0.704	5.53		
					0.743	5.85				
Mo2–CO	0.715	5.56			0.739	5.85	0.715	5.44		
					0.702	5.58				
C–O	2.793	17.63			2.714	14.90	2.793	17.72		
					2.713	14.84				

<sup>a</sup> Values of the electron density at the bond critical points ( $\rho$ ) are given in  $\text{e} \text{Å}^{-3}$ ; values of the Laplacian of the electron density at these points ( $\nabla^2\rho$ ) are given in  $\text{e} \text{Å}^{-5}$ ; the Mo1 label corresponds to the metal atom positioned away from the methyl group of the methoxycarbonyl ligand, except for compounds 2, A, and 7, for which both metal centers are equivalent; C\* refers to the bridgehead atom of the carbonyl ligand.

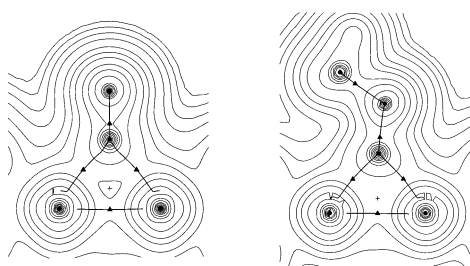


Figure 6. Electron density maps of complex 3 in the planes Mo–C(O)–Mo (left) and Mo–C(OMe)–Mo (right). Nuclear positions (●), bond critical points (▲), bond critical paths (bold lines), and ring critical points (+) are also indicated.

Table 5. Properties of the Electron Density in Some Prototypical Dinuclear Complexes<sup>a</sup>

compd	BO <sup>b</sup>	$\Delta_{M-M}/\text{Å}$	$r$	$\nabla^2\rho$
[Mo <sub>2</sub> (HCO <sub>2</sub> ) <sub>4</sub> ]	4	2.122	1.186	13.34
[Mo <sub>2</sub> Me <sub>6</sub> ]	3	2.212	0.996	10.08
[Mo <sub>2</sub> (NMe <sub>2</sub> ) <sub>6</sub> ]	3	2.243	0.962	8.37
[Mo <sub>2</sub> Cp <sub>2</sub> (CO) <sub>4</sub> ]	3	2.519	0.576	2.51
[Mo <sub>2</sub> (CO) <sub>10</sub> ] <sup>2-</sup>	1	3.334	0.140	0.29
[Mo <sub>2</sub> Cp <sub>2</sub> (CO) <sub>6</sub> ]	1	3.343	0.171	0.21

<sup>a</sup> Values of the electron density at the intermetallic bond critical points ( $\rho$ ) are given in  $\text{e} \text{Å}^{-3}$ ; values of the Laplacian of the electron density at these points ( $\nabla^2\rho$ ) are given in  $\text{e} \text{Å}^{-5}$ . <sup>b</sup> Formal order of the intermetallic bond.

significant multiplicity in the C–O bond, consistent with the MO analysis made above, but the figures cannot be fully compared due to the differences in the carbon environments (trigonal vs tetrahedral) and the implied geometrical effects, already noticed. However, we must note that the distinct types of C–O bonds also exhibit quite different values of the Laplacian of  $\rho$  at the corresponding bcp's. For the carbonyl bridges this function takes quite high and positive values ( $17.72 > \nabla^2\rho > 14.84 \text{ e} \text{Å}^{-5}$ ), whereas these values are still positive, but much lower, for the C(carbyne)–O bonds ( $0.88 > \nabla^2\rho > 1.89 \text{ e} \text{Å}^{-5}$ ), and finally the O–Me bonds have values of  $\nabla^2\rho$  as expected from covalent bonds, that is, with figures that are negative ( $-8.19 > \nabla^2\rho > -10.38 \text{ e} \text{Å}^{-5}$ ). Actually, the latter are not very different from those previously reported for simple organic molecules such as dimethyl ether ( $\nabla^2\rho = -9.94 \text{ e} \text{Å}^{-5}$ ).<sup>39</sup> The presence of positive values is a characteristic of the carbonyl ligands coordinated to metal atoms, being derived from their singular electron distribution, and in the free molecule

this function exhibits an even higher value ( $\nabla^2\rho = 20.29 \text{ e} \text{Å}^{-5}$ ).<sup>39</sup> We trust that the above differences in the values of the Laplacian of the electron density at the C–O bcp's are another indication of the persistence of significant  $\pi$ -bonding interaction in the corresponding bond of the methoxycarbonyl ligand.

### Concluding Remarks

The carbonyl-bridged complexes 1 to 4 react with either [Me<sub>3</sub>O]BF<sub>4</sub> or HBF<sub>4</sub>·OEt<sub>2</sub> to give the corresponding methoxy- or hydroxycarbonyl derivatives 5 to 8 as a result of a charge-controlled addition of the electrophile at the oxygen atom of the carbonyl bridges. The DFT method used in all these complexes leads to face-sharing bioctahedral optimized geometries that are in excellent agreement with those experimentally determined through X-ray diffraction. The analysis of the molecular orbitals in these 30-electron complexes gives support to the triple intermetallic bond proposed according to the EAN rule, which is made up of one  $\sigma$  and two  $\delta$  components; the latter orbitals, however, are involved in  $\pi$  back-bonding with the bridging carbonyls and, to a greater extent, in  $\pi$  bonding with the carbonyl ligands. These two interactions imply a delocalization of the bonding electrons over the Mo<sub>2</sub>C triangles and thus a partial reduction of the direct intermetallic binding. In addition, in the methoxycarbonyl complexes there is some residual  $\pi$ -bonding interaction at the C–O bond of the carbonyl ligand (originally a bridging carbonyl), which competes with the metal–carbonyl  $\pi$  bonding. The topological analysis of the electron density within these unsaturated molecules is fully consistent with the MO description of the bonding just given. The electron density at the intermetallic bond critical points decreases only slightly upon methylation of the carbonyl bridges and still keeps a high value of ca.  $0.6 \text{ e} \text{Å}^{-3}$ , comparable to that calculated for the triply bonded [Mo<sub>2</sub>Cp<sub>2</sub>(CO)<sub>4</sub>]. At the same time, the electron densities at the Mo–C (carbonyl) bcp's (ca.  $0.88 \text{ e} \text{Å}^{-3}$  on average) are substantially increased above the figures for the Mo–C(carbyne) bonds (ca.  $0.71 \text{ e} \text{Å}^{-3}$ ), in agreement with the increased order of those Mo–C bonds. Yet, the persistence of substantial multiplicity in the C(carbyne)–O bond of the methoxycarbonyl ligand in the complexes studied can be clearly deduced from the values of electron density and their Laplacian at the corresponding bcp's, which are intermediate between the corresponding figures of the bridging carbonyls and those of the methoxyl groups.

## Experimental Section

**General Procedures and Starting Materials.** All manipulations and reactions were carried out under a nitrogen (99.995%) atmosphere using standard Schlenk techniques. Solvents were purified according to literature procedures and distilled prior to use.<sup>41</sup> Petroleum ether refers to that fraction distilling in the range 65–70 °C. Compounds [W<sub>2</sub>Cp<sub>2</sub>(μ-PPh<sub>2</sub>)<sub>2</sub>(μ-CO)] (**1**),<sup>16</sup> [Mo<sub>2</sub>Cp<sub>2</sub>(μ-PEt<sub>2</sub>)<sub>2</sub>(μ-CO)] (**2**),<sup>16</sup> and [Mo<sub>2</sub>Cp<sub>2</sub>(μ-COR)(μ-PCy<sub>2</sub>)(μ-CO)] [R = Me (**3**), Et (**4**)]<sup>17</sup> were prepared as described previously. All other reagents were obtained from the usual commercial suppliers and used as received. Filtrations were carried out using diatomaceous earth. IR stretching frequencies were measured in solution or Nujol mulls and are referred to as ν(solvent) or ν(Nujol), respectively. Nuclear magnetic resonance (NMR) spectra were routinely recorded at 300.13 (<sup>1</sup>H), 121.50 (<sup>31</sup>P{<sup>1</sup>H}), or 75.47 (<sup>13</sup>C{<sup>1</sup>H}) at 290 K in CD<sub>2</sub>Cl<sub>2</sub> solutions unless otherwise stated. Chemical shifts (δ) are given in ppm, relative to internal tetramethylsilane (<sup>1</sup>H, <sup>13</sup>C) or external 85% aqueous H<sub>3</sub>PO<sub>4</sub> (<sup>31</sup>P). Coupling constants (*J*) are given in Hz.

**Preparation of [W<sub>2</sub>Cp<sub>2</sub>(μ-COMe)(μ-PPh<sub>2</sub>)<sub>2</sub>]BF<sub>4</sub> (**5**).** A dichloromethane solution (10 mL) of compound **1** (0.100 g, 0.112 mmol) was stirred with an excess of [Me<sub>3</sub>O]BF<sub>4</sub> (ca. 0.050 g, 0.34 mmol) for 2 h to give a brown solution. This solution was filtered, and then petroleum ether (15 mL) was added to this filtrate. Removal of the solvents under vacuum and washing of the residue with petroleum ether gave compound **5** as a brown powder (0.103 g, 92%). Anal. Calcd for C<sub>36</sub>H<sub>33</sub>BF<sub>4</sub>OP<sub>2</sub>W<sub>2</sub>: C, 43.32; H, 3.33. Found: C, 43.25; H, 3.39. IR ν(Nujol): 1281 (s, C–OMe), 1051 (s, br, B–F) cm<sup>-1</sup>. <sup>1</sup>H NMR: δ 8.0–7.1 (m, 20H, Ph), 6.30 (s, 10H, Cp), 4.06 (s, 3H, OCH<sub>3</sub>) ppm.

**Preparation of [Mo<sub>2</sub>Cp<sub>2</sub>(μ-COMe)(μ-PEt<sub>2</sub>)<sub>2</sub>]BF<sub>4</sub> (**6**).** The procedure is identical to that described for **5**, but using compound **2** (0.300 g, 0.568 mmol) instead. This gives compound **6** (0.347 g, 97%) as a brown powder. Anal. Calcd for C<sub>20</sub>H<sub>33</sub>BF<sub>4</sub>Mo<sub>2</sub>OP<sub>2</sub>: C, 38.12; H, 5.28. Found: C, 38.23; H, 5.40. IR ν(Nujol): 1271 (s, C–O), 1045 (s, br, B–F) cm<sup>-1</sup>. <sup>1</sup>H NMR: δ 6.01 (s, 10H, Cp), 3.85 (s, 3H, OCH<sub>3</sub>), 2.17 (m, 4H, PCH<sub>2</sub>), 2.00 (m, 4H, PCH<sub>2</sub>), 1.10, 0.34 (2 × dt, *J*<sub>HP</sub> = 18, *J*<sub>HH</sub> = 8, 2 × 6H, CH<sub>3</sub>) ppm. <sup>13</sup>C{<sup>1</sup>H} NMR: δ 367.9 (t, *J*<sub>CP</sub> = 14, μ-COMe), 93.8 (s, Cp), 68.6 (s, OCH<sub>3</sub>), 36.5 (m, AA'X, 2 × PCH<sub>2</sub>), 31.2 (false t, AA'X, |*J*<sub>CP</sub> + *J*<sub>CP</sub>| = 9, 2 × PCH<sub>2</sub>), 13.0 (s, 2 × CH<sub>3</sub>), 10.5 (s, 2 × CH<sub>3</sub>) ppm.

**Preparation of [Mo<sub>2</sub>Cp<sub>2</sub>(μ-COMe)<sub>2</sub>(μ-PCy<sub>2</sub>)<sub>2</sub>]BF<sub>4</sub> (**7**).** The procedure is identical to that described for **5**, but using compound **3** (0.100 g, 0.169 mmol) instead. This gives compound **7** (0.107 g, 92%) as a brown powder. Anal. Calcd for C<sub>26</sub>H<sub>38</sub>BF<sub>4</sub>Mo<sub>2</sub>O<sub>2</sub>P·CH<sub>2</sub>Cl<sub>2</sub>: C, 41.72; H, 5.18. Found: C, 41.68; H, 5.25. IR ν(Nujol): 1308 (w, C–O<sub>asym</sub>), 1273 (s, C–O<sub>sym</sub>) cm<sup>-1</sup>. <sup>1</sup>H NMR: δ 6.22 (s, 10H, Cp), 4.00 (s, 6H, OCH<sub>3</sub>), 2.1–0.4 (m, 22H, Cy) ppm. <sup>13</sup>C{<sup>1</sup>H} NMR: δ 366.0 (d, *J*<sub>CP</sub> = 13, μ-COMe), 97.1 (s, Cp), 69.4 (s, OMe), 40.5 [d, *J*<sub>CP</sub> = 17, C<sup>1</sup>(Cy)], 33.5 [s, C<sup>2</sup>(Cy)], 27.1 [d, *J*<sub>CP</sub> = 13, C<sup>3</sup>(Cy)], 25.9 [s, C<sup>4</sup>(Cy)] ppm.

**Preparation of [Mo<sub>2</sub>Cp<sub>2</sub>(μ-COEt)(μ-COMe)(μ-PCy<sub>2</sub>)<sub>2</sub>]BF<sub>4</sub> (**8**).** The procedure is identical to that described for **5**, but using compound **4** (0.100 g, 0.165 mmol) instead. This gives compound **8** as a brownish-yellow powder (0.109 g, 94%). Anal. Calcd for C<sub>27</sub>H<sub>40</sub>BF<sub>4</sub>Mo<sub>2</sub>O<sub>2</sub>P: C, 45.92; H, 5.71. Found: C, 45.99; H, 5.61. <sup>1</sup>H NMR: δ 6.21 (s, 10H, Cp), 4.20 (q, *J*<sub>HH</sub> = 7, 2H, OCH<sub>2</sub>), 4.00 (s, 3H, OCH<sub>3</sub>), 1.43 (t, *J*<sub>HH</sub> = 7, 3H, CH<sub>3</sub>), 2.1–0.4 (m, 22H, Cy) ppm. <sup>13</sup>C{<sup>1</sup>H} NMR: δ 365.7 (d, *J*<sub>CP</sub> = 13, μ-COR), 363.5 (d, *J*<sub>CP</sub> = 13, μ-COR), 96.9 (s, Cp), 80.4 (s, OCH<sub>2</sub>), 69.2 (s, OCH<sub>3</sub>), 40.3 [d, *J*<sub>CP</sub> = 18, C<sup>1</sup>(Cy)], 33.2 [s, C<sup>2</sup>(Cy)], 26.8 [d, *J*<sub>CP</sub> = 15, C<sup>3</sup>(Cy)], 25.7 [s, C<sup>4</sup>(Cy)], 14.6 (s, CH<sub>3</sub>) ppm.

**Preparation of Solutions of [Mo<sub>2</sub>Cp<sub>2</sub>(μ-COH)(μ-PEt<sub>2</sub>)<sub>2</sub>]BF<sub>4</sub> (**9**).** Compound **2** (0.030 g, 0.057 mmol) and HBF<sub>4</sub>·OEt<sub>2</sub> (8 μL of

a 54% Et<sub>2</sub>O solution, 0.06 mmol) were stirred in CH<sub>2</sub>Cl<sub>2</sub> (5 mL) or CD<sub>2</sub>Cl<sub>2</sub> (0.6 mL) at 243 K for 2 min to give brownish solutions shown (by NMR) to contain essentially pure compound **9**. These solutions decomposed progressively upon storage or manipulation above ca. 273 K to give compound **11** and then other yet uncharacterized products. Spectroscopic data for compound **9**: <sup>1</sup>H NMR (243 K): δ 12.65 (s, br, 1H, COH), 5.96 (s, 10H, Cp), 2.12 (m, 4H, CH<sub>2</sub>), 2.02 (m, 4H, CH<sub>2</sub>), 1.06 (dt, *J*<sub>HP</sub> = 17, *J*<sub>HH</sub> = 7, 6H, CH<sub>3</sub>), 0.31 (dt, *J*<sub>HP</sub> = 20, *J*<sub>HH</sub> = 7, 6H, CH<sub>3</sub>) ppm. <sup>13</sup>C{<sup>1</sup>H} NMR (213 K): δ 368.9 (t, *J*<sub>CP</sub> = 11, μ-COH), 94.0 (s, Cp), 36.4 (m, AA'X, |*J*<sub>CP</sub> + *J*<sub>CP</sub>| = 27, 2 × CH<sub>2</sub>), 30.0 (m, AA'X, |*J*<sub>CP</sub> + *J*<sub>CP</sub>| = 16, 2 × CH<sub>2</sub>), 13.9 (s, 2 × CH<sub>3</sub>), 10.6 (s, 2 × CH<sub>3</sub>) ppm. Spectroscopic data for compound **11**: IR ν(CH<sub>2</sub>Cl<sub>2</sub>) 1843 (C–O) cm<sup>-1</sup>. <sup>1</sup>H NMR: δ 5.75 (s, 10H, Cp), 2.49 (m, 4H, PCH<sub>2</sub>), 2.04 (m, 4H, PCH<sub>2</sub>), 1.32 (dt, *J*<sub>HP</sub> = 18, *J*<sub>HH</sub> = 7, 6H, CH<sub>3</sub>), 0.73 (dt, *J*<sub>HP</sub> = 20, *J*<sub>HH</sub> = 8, 6H, CH<sub>3</sub>), -1.21 (t, *J*<sub>HP</sub> = 45, 1H, Mo–H) ppm. <sup>1</sup>H NMR (253 K): δ 5.76 (s, br, 10H, Cp), 2.63 (s, br, 2H, PCH<sub>2</sub>), 2.31 (s, br, 2H, PCH<sub>2</sub>), 2.06 (s, br, 4H, PCH<sub>2</sub>), 1.31 (dt, *J*<sub>HP</sub> = 18, *J*<sub>HH</sub> = 7, 6H, CH<sub>3</sub>), 0.70 (dt, *J*<sub>HP</sub> = 20, *J*<sub>HH</sub> = 8, 6H, CH<sub>3</sub>), -1.34 (t, *J*<sub>HP</sub> = 45, 1H, Mo–H) ppm. <sup>1</sup>H NMR (213 K): δ 5.83 (s, 5H, Cp), 5.73 (s, 5H, Cp), 2.69 (s, br, 2H, PCH<sub>2</sub>), 2.19 (s, br, 2H, PCH<sub>2</sub>), 1.99 (s, br, 4H, PCH<sub>2</sub>), 1.31 (m, br, 6H, CH<sub>3</sub>), 0.65 (m, br, 6H, CH<sub>3</sub>), -1.47 (t, *J*<sub>HP</sub> = 45, 1H, Mo–H) ppm. <sup>13</sup>C{<sup>1</sup>H} NMR (213 K): δ 259.8 (t, *J*<sub>CP</sub> = 7, CO), 94.5 (s, Cp), 92.5 (s, Cp), 37.4 (m, AA'X, |*J*<sub>CP</sub> + *J*<sub>CP</sub>| = 28, 2 × PCH<sub>2</sub>), 31.9 (m, AA'X, 2 × PCH<sub>2</sub>), 13.4 (s, 2 × CH<sub>3</sub>), 12.9 (s, 2 × CH<sub>3</sub>) ppm.

**Preparation of Solutions of [Mo<sub>2</sub>Cp<sub>2</sub>(μ-COH)(μ-COMe)(μ-PCy<sub>2</sub>)<sub>2</sub>]BF<sub>4</sub> (**10**).** Compound **3** (0.030 g, 0.05 mmol) and HBF<sub>4</sub>·OEt<sub>2</sub> (8 μL of a 54% Et<sub>2</sub>O solution, 0.06 mmol) were stirred in CH<sub>2</sub>Cl<sub>2</sub> (5 mL) or CD<sub>2</sub>Cl<sub>2</sub> (0.6 mL) at 233 K for 2 min to give yellow solutions shown (by NMR) to contain essentially pure compound **10**. These solutions decomposed progressively upon storage or manipulation above ca. 253 K to give compound **12** and then other yet uncharacterized products. Spectroscopic data for compound **10**: <sup>1</sup>H NMR (233 K): δ 13.16 (s, br, 1H, COH), 6.18 (s, 10H, Cp), 3.94 (s, 3H, OMe), 2.2–0.3 (m, 22H, Cy) ppm. <sup>13</sup>C{<sup>1</sup>H} NMR (233 K): δ 365.8 (d, br, *J*<sub>CP</sub> = 13, μ-COH), 363.0 (d, *J*<sub>CP</sub> = 13, μ-COMe), 97.1 (s, Cp), 68.9 (s, OCH<sub>3</sub>), 40.1 [d, *J*<sub>CP</sub> = 18, C<sup>1</sup>(Cy)], 39.0 [d, *J*<sub>CP</sub> = 18, C<sup>1</sup>(Cy)], 33.4 [s, 4 × C<sup>2</sup>(Cy)], 26.98 [d, *J*<sub>CP</sub> = 12, 2 × C<sup>3</sup>(Cy)], 26.95 [d, *J*<sub>CP</sub> = 12, 2 × C<sup>3</sup>(Cy)], 25.79, 25.74 [2 × s, 2 × C<sup>4</sup>(Cy)] ppm. Spectroscopic data for compound **12**: ν(CH<sub>2</sub>Cl<sub>2</sub>) 1873 (C–O) cm<sup>-1</sup>. <sup>1</sup>H NMR (243 K): δ 6.00 (s, 5H, Cp), 5.91 (s, 5H, Cp), 4.16 (s, 3H, OCH<sub>3</sub>), 2.1–0.4 (m, 22H, Cy), -1.40 (d, *J*<sub>HP</sub> = 32, 1H, Mo–H) ppm. <sup>31</sup>P{<sup>1</sup>H} NMR (243 K): δ 294.5 (s) ppm.

**Computational Details.** All computations were carried out using the GAUSSIAN03 package,<sup>42</sup> in which the hybrid method B3LYP was applied with the Becke three-parameter exchange functional<sup>43</sup> and the Lee–Yang–Parr correlation functional.<sup>44</sup> Effective core potentials (ECP) and their associated double-ζ LANL2DZ basis set were used for the molybdenum and phosphorus atoms,<sup>45</sup>

(42) Frisch, M. J.; Trucks, G. W.; Schlegel, H. B.; Scuseria, G. E.; Robb, M. A.; Cheeseman, J. R.; Montgomery, J. A., Jr.; Vreven, T.; Kudin, K. N.; Burant, J. C.; Millam, J. M.; Iyengar, S. S.; Tomasi, J.; Barone, V.; Mennucci, B.; Cossi, M.; Scalmani, G.; Rega, N.; Petersson, G. A.; Nakatsuji, H.; Hada, M.; Ehara, M.; Toyota, K.; Fukuda, R.; Hasegawa, J.; Ishida, M.; Nakajima, T.; Honda, Y.; Kitao, O.; Nakai, H.; Klene, M.; Li, X.; Knox, J. E.; Hratchian, H. P.; Cross, J. B.; Bakken, V.; Adamo, C.; Jaramillo, J.; Gomperts, R.; Stratmann, R. E.; Yazyev, O.; Austin, A. J.; Cammi, R.; Pomelli, C.; Ochterski, J. W.; Ayala, P. Y.; Morokuma, K.; Voth, G. A.; Salvador, P.; Dannenberg, J. J.; Zakrzewski, V. G.; Dapprich, S.; Daniels, A. D.; Strain, M. C.; Farkas, O.; Malick, D. K.; Rabuck, A. D.; Raghavachari, K.; Foresman, J. B.; Ortiz, J. V.; Cui, Q.; Baboul, A. G.; Clifford, S.; Cioslowski, J.; Stefanov, B. B.; Liu, G.; Liashenko, A.; Piskorz, P.; Komaromi, I.; Martin, R. L.; Fox, D. J.; Keith, T.; Al-Laham, M. A.; Peng, C. Y.; Nanayakkara, A.; Challacombe, M.; Gill, P. M. W.; Johnson, B.; Chen, W.; Wong, M. W.; Gonzalez, C.; and Pople, J. A. *Gaussian 03*, Revision B.02; Gaussian, Inc.: Wallingford, CT, 2004.

(43) Becke, A. D. *J. Chem. Phys.* **1993**, *98*, 5648.

(44) Lee, C.; Yang, W.; Parr, R. G. *Phys. Rev. B* **1988**, *37*, 785.

(41) Amarego, W. L. F.; Chai, C. *Purification of Laboratory Chemicals*, 5th ed.; Butterworth-Heinemann: Oxford, UK, 2003.



supplemented by an extra d-polarization function in the case of P.<sup>46</sup> The light elements (O, C, and H) were described with the 6-31G\* basis.<sup>47</sup> Geometry optimizations were performed under no symmetry restrictions, using initial coordinates derived from X-ray data of the same or comparable complexes, and frequency analyses were performed to ensure that a minimum structure with no imaginary frequencies was achieved in each case. In the case of complexes **6** and **7**, the geometry optimization converged with one negative vibrational frequency of low value (ca. 10i cm<sup>-1</sup>), which was assigned to the internal rotation of one of the cyclopentadienyl ligands. At this point we did not follow the imaginary eigenvector in search of a stationary point with no imaginary vibrational frequencies. In all other cases, imaginary frequencies were absent. For interpretation purposes, natural population analysis (NPA) charges<sup>28b</sup> were derived from the natural bond order (NBO) analysis

(45) Hay, P. J.; Wadt, W. R. *J. Chem. Phys.* **1985**, *82*, 299.

(46) Höllwarth, A.; Böhme, M.; Dapprich, S.; Ehlers, A. W.; Gobbi, A.; Jonas, V.; Köhler, K. F.; Stegman, R.; Veldkamp, A.; Frenking, G. *Chem. Phys. Lett.* **1993**, *208*, 237.

(47) (a) Hariharan, P. C.; Pople, J. A. *Theor. Chim. Acta* **1973**, *28*, 213. (b) Petersson, G. A.; Al-Laham, M. A. *J. Chem. Phys.* **1991**, *94*, 6081. (c) Petersson, G. A.; Bennett, A.; Tensfeldt, T. G.; Al-Laham, M. A.; Shirley, W. A.; Mantzaris, J. *J. Chem. Phys.* **1988**, *89*, 2193.

of the data.<sup>28b</sup> Molecular orbitals and vibrational modes were visualized using the Molekel program.<sup>48</sup> The topological analysis of the electron density  $\rho$  was carried out with the Xaim routine.<sup>49</sup>

**Acknowledgment.** We thank the MEC of Spain for a grant (to D.G.) and financial support (Projects BQU2003-05471 and CTQ2005-08123-C02-02BQU). The computing resources at the Centre de Supercomputació de Catalunya (CESCA) were made available to us through a grant from Fundació Catalana per a la Recerca (FCR) and Universitat de Barcelona.

**Supporting Information Available:** Mulliken and NPA charges, molecular orbitals, and data from the AIM topological analysis for complexes **2**, **3**, **A**, **6**, and **7**. This material is available free of charge via the Internet at <http://pubs.acs.org>.

OM700562G

(48) Portmann, S.; Lüthi, H. P. MOLEKEL: An Interactive Molecular Graphics Tool. *CHIMIA* **2000**, *54*, 766.

(49) Ortiz, J. C.; Bo, C. *Xaim*; Departamento de Química Física e Inorgánica, Universidad Rovira i Virgili: Tarragona, Spain, 1998.

(50) Adatia, T.; McPartlin, M.; Mays, M. J.; Morris, M. J.; Raithby, P. R. *J. Chem. Soc., Dalton Trans.* **1989**, 1555.